cell regeneration observed in adult recovery from bone-marrow aplasia that is mainly composed of memory CD4$^+$ T cells (*18*). The trend toward normalization of CD4$^+$ T cells displaying the CD28 costimulatory molecule (*8*) observed in our studies reflects the lower CD4$^+$ T cell activation and might allow for some recovery from enhanced sensitivity to apoptosis or anergy (*19*). The loss of memory CD4$^+$ T cell reactivity to recall antigens was indeed reversible under efficient antiviral therapy. This latter observation contrasts with the limited benefit for CD4$^+$ T cell function reported with ritonavir alone, where a weaker reduction in viral load (–1 log) could only increase preexisting CD4$^+$ T cell responses but failed to restore a lost T cell reactivity to recall antigens (*20*). The significant but partial restoration of CD4$^+$ T cell proliferation to recall antigens that we report might participate to the progressive regeneration of mature peripheral CD4$^+$ T cells observed after the first month of treatment, in agreement with murine models (*21, 22*).

This sequence of events suggests that, in the natural course of a productive infection, HIV activity per se is the driving force for chronic immune stimulation; the latter would take part in the defects in antigen-specific CD4$^+$ T cell activation and proliferation noted in HIV-infected patients (*6, 7*). Because such functions are required for a normal homeostasis of mature peripheral T cells in adults (*21*), their alteration would appear as a key mechanism in HIV-induced CD4$^+$ T cell depletion. This impairment of the mature CD4$^+$ cell repopulation process was, in part, reversible under effective antiviral treatment, although the balance between CD4$^+$ and CD8$^+$ subsets was not yet normalized with CD8$^+$ counts still higher than normal and CD4$^+$ counts remaining below normal thresholds. Earlier or stronger therapeutic interventions should reasonably achieve better reversibility.

REFERENCES AND NOTES

1. M. Markowitz *et al.*, *N. Engl. J. Med.* **333**, 1534 (1995); R. Gulick *et al.*, in *Third National Conference on Human Retroviruses and Related Diseases*, Washington, DC, 28 January to 1 February 1996; A. C. Collier *et al.*, *N. Engl. J. Med.* **334**, 1011 (1996); D. Mathez *et al.*, *Antiretroviral Ther.*, in press.
2. W. Wei *et al.*, *Nature* **373**, 117 (1995); D. D. Ho *et al.*, *ibid.*, p. 123.
3. D. E. Mosier *et al.*, *ibid.* **375**, 193 (1995).
4. R. B. Effros *et al.*, *AIDS* **10**, F17 (1996); K. C. Wolthers *et al.*, *Science* **274**, 1543 (1996).
5. M. Roederer *et al.*, *J. Clin. Invest.* **95**, 2061 (1995).
6. J. V. Giorgi, *Immunology of HIV Infection* (Plenum, New York, 1996), p. 181.
7. H. C. Lane *et al.*, *N. Engl. J. Med.* **313**, 79 (1985); J. V. Giorgi *et al.*, *J. Immunol.* **138**, 3725 (1987); M. Clerici *et al.*, *J. Clin. Invest.* **82**, 1908 (1988).
8. B. Autran *et al.*, data not shown.
9. M. Merklenslager *et al.*, *Eur. J. Immunol.* **18**, 1653 (1988).
10. T. F. Tedder *et al.*, *J. Immunol.* **134**, 2989 (1985).
11. S. S. Kansas, *Blood* **88**, 3259 (1996).
12. S. M. Schnittman *et al.*, *Proc. Natl. Acad. Sci. U.S.A.* **87**, 6058 (1990).
13. T. Hara *et al.*, *J. Exp. Med.* **164**, 1988 (1986).
14. M. Levacher *et al.*, *Clin. Exp. Immunol.* **90**, 376 (1992); J. V. Giorgi *et al.*, *J. Acquired Immune Defic. Syndr.* **6**, 904 (1993); M. Bofill *et al.*, *AIDS* **10**, 827 (1996).
15. J. Sprent, *Curr. Opin. Immunol.* **5**, 433 (1993); D. F. Tough *et al.*, *Immunol. Rev.* **150**, 129 (1996).
16. C. Aussel *et al.*, *Cell. Immunol.* **155**, 436 (1994).
17. W. Cavert *et al.*, Science **276**, 960 (1997).
18. C. L. Mackall *et al.*, *N. Engl. J. Med.* **332**, 143 (1995).
19. N. J. Borthwick *et al.*, *AIDS* **8**, 431 (1994).
20. A. D. Kelleher *et al.*, *J. Infect. Dis.* **173**, 321 (1996).
21. B. Rocha and H. von Boehmer, *Science* **251**, 1225 (1991).
22. C. Tanchot and B. Rocha, *Eur. J. Immunol.* **25**, 2127 (1995).
23. D. Mathez *et al.*, *Antimicrob. Agents Chemother.* **37**, 2206 (1993).
24. B. Autran *et al.*, *J. Immunol.* **154**, 1408 (1995).

25. We thank the clinicians participating in the therapeutic trial: A. G. Saimot, I. Gorin, G. Pialoux, and P. De Truchis; V. Calvez for analyzing HIV-1 plasma viral load; J. P. Chauvin from Abbott Laboratories for sponsoring the clinical trial; D. Faudot and M. Hirn from Coulter/Immunotech for kindly providing reagents; and SIDACTION and the Agence Nationale de Recherches sur le SIDA for financial support.

12 February 1997; accepted 7 May 1997

Chemical Coupling Between Atmospheric Ozone and Particulate Matter

Z. Meng, D. Dabdub, J. H. Seinfeld*

A major fraction of ambient particulate matter arises from atmospheric gas-to-particle conversion. Attempts to reduce particulate matter levels require control of the same organic and nitrogen oxide (NO_x) emissions that are precursors to urban and regional ozone formation. Modeling of the gas-aerosol chemical interactions that govern levels of particulate components showed that control of gas-phase organic and NO_x precursors does not lead to proportionate reductions of the gas-phase–derived components of atmospheric particles. The chemical coupling between ozone and particulate matter has implications for strategies to achieve the new ozone and particulate matter standards proposed by the U.S. Environmental Protection Agency.

Ozone has historically been regarded as the principal urban and regional air quality problem in the United States (*1*). Epidemiological evidence that urban mortality rates are correlated with mass concentration of fine particulate matter has now focused intense interest on reducing levels of airborne particles (*2*). In November 1996, the U.S. Environmental Protection Agency (EPA) proposed new ozone (O_3) and particulate matter air quality standards (*3*). Because exposure to lower O_3 concentrations over longer periods of time than the current standard (0.12 parts per million averaged over a 1-hour period) is deemed to be of primary relevance, EPA proposed to lower the O_3 standard to 0.08 ppm averaged over an 8-hour period. EPA also proposed to revise the existing particulate matter (PM) standard to add two new $PM_{2.5}$ (particulate matter of diameter less than or equal to 2.5 μm) standards set at 15 $\mu g\ m^{-3}$ for the annual mean, and 50 $\mu g\ m^{-3}$ over a 24-hour period. Hundreds of counties in the United States in addition to those already in violation of the current standards are estimated to violate either or both of the new O_3 and PM standards (*4*).

Ozone and PM have traditionally been considered as separate problems. However, O_3 and PM are chemically coupled, and this coupling is of profound importance in understanding processes that control the levels of both. Urban and regional ozone abatement strategies have, for more than a decade, been evaluated with three-dimensional atmospheric models by the EPA and state and local agencies (*1*). We report here the application of a three-dimensional, size- and chemically resolved gas-aerosol model to examine how the chemical coupling that exists between O_3 and PM influences joint control of the two classes of pollutants.

The common components of atmospheric particles, such as sulfate (SO_4^{2-}), nitrate (NO_3^-), ammonium (NH_4^+), organic compounds, crustal material, and water, reach the particulate phase by several different processes (Fig. 1). Aside from the direct emission of particles into the atmosphere, gas-to-particle conversion processes play an essential role in determining the mass of airborne PM. Such processes depend intimately on the organic

Z. Meng, Department of Environmental Engineering Science, California Institute of Technology, Pasadena, CA 91125, USA.
D. Dabdub, Department of Mechanical and Aerospace Engineering, University of California, Irvine, CA 92717–3975, USA.
J. H. Seinfeld, Department of Chemical Engineering and Division of Engineering and Applied Science, California Institute of Technology, Pasadena, CA 91125, USA.

---

*To whom correspondence should be addressed. E-mail: john_seinfeld@starbase1.caltech.edu and NO_x gas-phase chemistry that generates ozone (Fig. 2). Gas-phase organic and NO_x chemistry is driven by the hydroxyl (OH) radical, the levels of which depend on the mixture of organics and the organic/NO_x relative concentrations (*5*). Gas-phase conversion of SO_2 to aerosol sulfate occurs by means of the reaction SO_2 + OH, which leads to H_2SO_4 vapor molecules that rapidly transfer to the particulate phase by nucleation or condensation on existing aerosol surfaces (*6, 7*). In the presence of fogs or clouds, aqueous-phase conversion of SO_2 to sulfate takes place, for example, by dissolved hydrogen peroxide (H_2O_2) or O_3 (*8*), and H_2O_2 concentrations depend indirectly on the OH concentration. Hydrogen peroxide is itself a gas-phase product of the HO_2-HO_2 reaction. A dominant termination reaction in the photochemical O_3 system is the production of nitric acid

$$OH + NO_2 \longrightarrow HNO_3 \tag{1}$$

As the most ubiquitous basic gas in the atmosphere, ammonia provides a route for the formation of particulate-phase nitrate by means of the reversible reaction (*9*)

$$NH_3(g) + HNO_3(g) \rightleftarrows NH_4NO_3(p) \tag{2}$$

where (g) denotes gas phase and (p) denotes particulate phase. Secondary organic aerosol results when a parent organic molecule A reacts with OH, O_3, or NO_3 to yield semivolatile products that partition themselves between the gas and aerosol phases (*10*).

The major gas-phase sinks of NO_x are HNO_3 and peroxyacetyl nitrate (PAN), $CH_3C(O)OONO_2$. Because of its reversible formation through reaction of peroxyacetyl radicals $CH_3C(O)OO\cdot$(sometimes denoted RCO_3) and NO_2,

$$CH_3C(O)OO\cdot + NO_2 \rightleftarrows CH_3C(O)OONO_2 \tag{3}$$

PAN serves as a temporary NO_x reservoir. Once formed, HNO_3 may either be removed by deposition or, in the presence of NH_3, form particulate NH_4NO_3. Gas-phase photochemistry determines the relative amounts of HNO_3 and PAN formed, and the amount of NH_3 present governs the subsequent split between HNO_3 loss by deposition and particulate NH_4NO_3 formation.

Gas-phase HNO_3 has a relatively high affinity to deposit on virtually any surface, a process termed dry deposition. A layer of HNO_3 uniformly distributed up to a height of 1 km has a half-life as a result of dry deposition of about 30 hours (*11*). Particulate NH_4NO_3, on the other hand, has an affinity for dry deposition that is about an order of magnitude less than that of HNO_3 (*12*). Consequently, for a layer of NH_4NO_3 particles uniformly distributed up to a height of 1 km, the half-life is an order of magnitude larger than that of HNO_3 vapor. In its role in converting HNO_3 to NH_4NO_3, ammonia therefore exerts a direct influence on the airborne lifetime of nitrate. At low NH_3 concentrations, more of the nitrate remains in the gas phase as HNO_3, where it is subject to dry deposition. In contrast, at higher concentrations of NH_3, more of the total nitrate is converted to particulate NH_4NO_3, and because of the lower dry deposition rate of particles, the overall atmospheric lifetime of nitrate is increased. As HNO_3 is removed by dry deposition, the $HNO_3/NH_3/NH_4NO_3$ equilibrium can be shifted back toward the gas phase, causing NH_4NO_3 to evaporate. Converting NH_4NO_3 back into HNO_3, which is subject to an enhanced rate of dry deposition, serves to shorten the overall atmospheric lifetime of oxidized nitrogen.

Three-dimensional urban and regional ozone models have been in existence for two decades (*13*). We report here on the application of a three-dimensional Eulerian urban and regional atmospheric model designed to study the dynamics of trace gases and aerosols (*14*). Gas-to-particle conver-

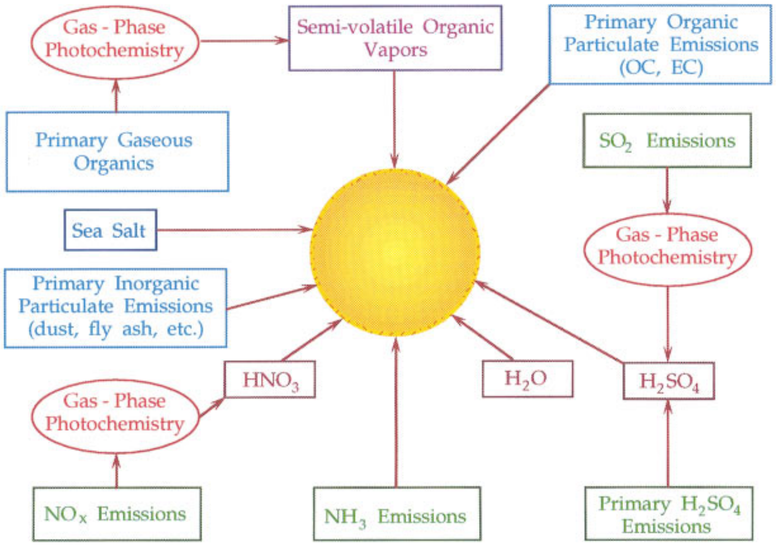

Fig. 1. Routes of incorporation of chemical species into atmospheric particulate matter. OC and EC denote organic and elemental carbon; other species are defined in the text.

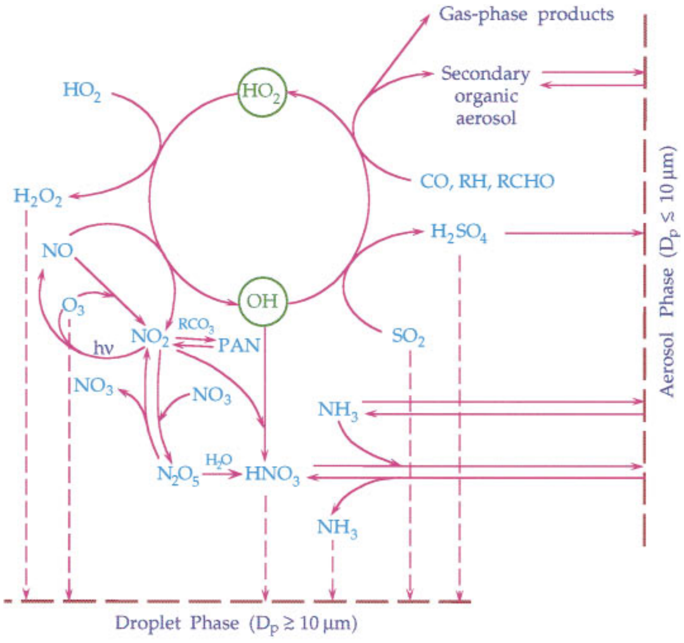

Fig. 2. Chemical coupling in the atmospheric gas, particle, and droplet phases. Cycling in the OH-HO_2 system generates tropospheric ozone (O_3) and hydrogen peroxide (H_2O_2), which are principal oxidants of dissolved SO_2. Hydroxyl (OH) levels determine the rates of oxidation of SO_2 and NO_2 to sulfuric and nitric acids, respectively, which are gas-phase precursors to aerosol sulfate and nitrate. Hydroxyl (and ozone) attack on organic molecules (denoted by RH in the figure, where R is an organic group) containing seven or more carbon atoms can generate semivolatile secondary organic aerosol. D_p is particle diameter and $h\nu$ is energy of a photon.

sion is represented by dynamic mass transfer between the gas and aerosol phases. The model uses an 80 × 30 rectangular master grid in the *x*, *y* plane. The computational domain corresponds to an irregular region within this grid composed of 994 columns of cells. Each column corresponds to a 5-km by 5-km region in the *x*, *y* plane and extends 1100 m in height. The columns are partitioned into five cells in the *z* direction. Each cell contains 40 gas-phase chemical species and 17 aerosol-phase species distributed over particle-size sections, between 0.04 and 10 μm in diameter.

Ambient particles generally consist of a mixture of volatile and nonvolatile components. Soil material is nonvolatile; elemental and organic carbonaceous species emitted directly from sources are also assumed to be nonvolatile. In the atmosphere the molecular transfer of volatile species such as HNO_3, NH_3, H_2O, and secondary organics between the gas and particulate phases tends to drive the overall gas-aerosol distribution of volatile species toward thermodynamic equilibrium. Water establishes equilibrium virtually instantaneously as compared with the characteristic time scale over which the aerosol is evolving, but theory shows that volatile inorganic species such as NH_4NO_3 may or may not achieve equilibrium rapidly, depending on the prevailing temperature, relative humidity, and aerosol surface area (*9*). Treatment of this approach to equilibrium for volatile species is an essential component of the gas-aerosol model (*15*).

The South Coast Air Basin of California (metropolitan Los Angeles), in spite of considerable improvements in air quality over the last two decades, continues to exhibit the most severe ozone and particulate matter air quality problem in the United States. For this reason, and because this region has the world's most extensive gas and particulate matter database against which to evaluate the performance of atmospheric models, we examined the chemical coupling between ozone and PM control in that area. We performed an extensive test of the performance of the model in simulating available data on gases and aerosols in the South Coast Air Basin from 27 to 28 August 1987, a period during the Southern California Air Quality Study (SCAQS) that experienced exceedingly high ozone and PM levels and for which a comprehensive gas-aerosol database exists (*16*).

Performance of the model in simulating the 27 to 28 August 1987 episode was analyzed by Meng *et al.* (*17*). Figure 3 shows the observed and predicted levels of O_3 and $PM_{2.5}$ NO_3^- at the Central Los Angeles and Riverside monitoring stations. A question critical to model application is the degree of uncertainty in predictions as a result of uncertainties in model inputs. It is well established that the most uncertain input in Los Angeles air pollution modeling is the volatile organic compound (VOC) inventory (*18*). Varying the total area-wide VOC emissions by ±25% produces little change in $PM_{2.5}$ levels, so input uncertainties do not appear to affect the use of the model to explore the phenomenology of joint control of ozone and PM.

The sensitivity of PM levels to emission reductions of organics and NO_x can be assessed by systematically changing source emissions by prescribed factors. We considered a matrix of control strategy cases (Table 1). Entries in the table indicate maxi-

Table 1. Maximum 1-hour average concentrations simulated at Riverside, California, on 28 August 1987 for various combinations of VOC and NO_x reduction from base estimated 1987 basinwide emissions. Numbers in parentheses are percentage changes compared with the base case. No NH_3 emission reduction is assumed.

NO_x reduction	Chemical species	VOC reduction		
		0%	25%	50%
0%	O_3 (ppb)	180*	146 (−19%)	119 (−34%)
	HNO_3 (ppb)	13.8*	16 (+17%)	16 (+17%)
	PAN (ppb)	13.7*	5.7 (−58%)	3.3 (−76%)
	$PM_{2.5}$ NO_3^- ($\mu g\ m^{-3}$)	97*	119 (+23%)	121 (+25%)
	$PM_{2.5}$ mass ($\mu g\ m^{-3}$)	146*	173 (+18%)	175 (+19%)
25%	O_3 (ppb)	175 (−2.6%)	172 (−4%)	170 (−6%)
	HNO_3 (ppb)	13.4 (−3%)	13.8 (0%)	13.6 (−1%)
	PAN (ppb)	14.3 (+4%)	13.6 (−1%)	13 (−6%)
	$PM_{2.5}$ NO_3^- ($\mu g\ m^{-3}$)	87 (−10%)	87 (−10%)	89 (−8%)
	$PM_{2.5}$ mass ($\mu g\ m^{-3}$)	133 (−9%)	134 (−9%)	137 (−7%)
50%	O_3 (ppb)	168 (−6%)	150 (−17%)	135 (−25%)
	HNO_3 (ppb)	11.5 (−17%)	8 (−42%)	8.5 (−39%)
	PAN (ppb)	14.4 (+5%)	8.6 (−37%)	6.2 (−55%)
	$PM_{2.5}$ NO_3^- ($\mu g\ m^{-3}$)	76 (−21%)	69 (−29%)	71 (−27%)
	$PM_{2.5}$ mass ($\mu g\ m^{-3}$)	120 (−18%)	133 (−9%)	124 (−15%)

*These entries are the model-simulated values at Riverside, California, on 28 August 1987 for the base-case emissions inventory. Correspondence between the simulated and measured values of O_3 and $PM_{2.5}$ NO_3^- is shown in Fig. 3. The maximum 1-hour average HNO_3 (13.8 parts per billion) occurred at noon. Measurements were reported as 4-hour averages; from noon to 4 p.m. the observed 4-hour average HNO_3 was 5.4 ppb, as compared with the predicted 4-hour average of 6.5 ppb. Maximum total measured $PM_{2.5}$ mass (4-hour average) was 120 $\mu g\ m^{-3}$, as compared with the maximum 1-hour average prediction of 146 $\mu g\ m^{-3}$.

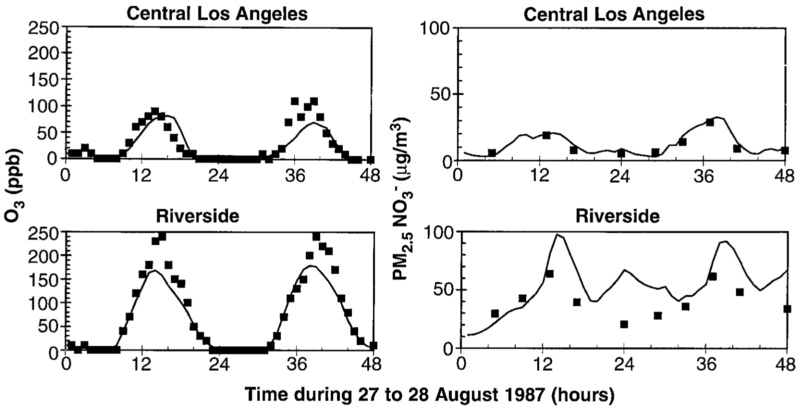

Fig. 3. Observed (data points) and predicted (solid line) concentrations of O_3 and $PM_{2.5}$ NO_3^- at downtown (central) Los Angeles and Riverside, California, on 27 to 28 August 1987.

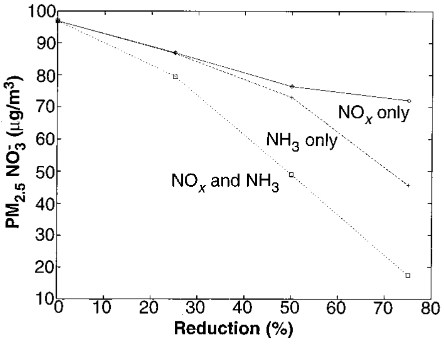

Fig. 4. Peak 1-hour average $PM_{2.5}$ nitrate levels achieved at Riverside, California, on 28 August 1987 as dependent on the degree of emissions reduction from the base conditions of the episode.

mum model- predicted levels of O_3, HNO_3, PAN, total $PM_{2.5}$ mass, and $PM_{2.5}$ nitrate mass at Riverside, California, on 28 August 1987. In these simulations, reductions in NH_3 base emissions were not considered. Reduction in NO_x emissions alone is predicted to lead to a slight decrease in peak 1-hour average O_3 levels. This behavior is consistent with the Basin being in an overall NO_x-rich state. Reductions in VOC emissions alone lead to more significant decreases in maximum O_3 levels than equivalent reductions in NO_x.

An important feature of the predicted response to VOC and NO_x reductions is the behavior of HNO_3, PAN, and $PM_{2.5}$ nitrate as either NO_x or VOC emissions are reduced. A 25% reduction in NO_x emissions at the base VOC level is predicted to lead to only a 3% reduction in peak HNO_3, a 4% increase in maximum PAN, and a 10% reduction in peak $PM_{2.5}$ nitrate; a 50% reduction in NO_x leads to a 5% increase in PAN and a 21% reduction in maximum $PM_{2.5}$ nitrate. When total NO_x is reduced, less NO_2 is available to produce either HNO_3 or PAN (reactions 1 and 3). If OH and RCO_3 radical levels remain unchanged as NO_x is decreased, reactions 1 and 3 predict that both HNO_3 and PAN should decrease accordingly. However, because HNO_3 decreases less than proportionately and PAN actually increases, decreases of NO_x lead to increases in both OH and RCO_3 levels, a behavior that is consistent with the region being in an NO_x-rich condition. If RCO_3 increases considerably more than OH, then PAN levels increase while HNO_3 levels exhibit a modest decrease, but one that is proportionately less than the NO_x reduction. As VOC levels are decreased, at any given NO_x level, PAN concentrations decrease as a result of the diminished availability of RCO_3 radicals. As less RCO_3 is available to convert NO_2 to PAN, more NO_2 is available to react with OH to form HNO_3 (though overall OH levels are less than in the base case). Because of this increase in HNO_3, $PM_{2.5}$ nitrate also increases. When production of RCO_3 cannot compensate for the NO_x reduction, PAN decreases also [compare PAN levels at each of 25 and 50% VOC control at 25 and 50% NO_x control (Table 1)]. Whereas our calculations are specific to the South Coast Air Basin of California, these conclusions can be expected to hold generally for any region having similar relative VOC/NO_x levels.

Maximum 1-hour $PM_{2.5}$ nitrate levels at Riverside for emission reductions of NO_x only, NH_3 only, and NO_x and NH_3 together (Fig. 4) illustrate the response of particulate nitrate levels to NH_3 emissions changes, which is indicative of the extent to which NH_3 controls the fixation of HNO_3 vapor to NH_4NO_3. For reductions of up to 50%, $PM_{2.5}$ nitrate reductions are essentially the same for individual reductions in NO_x or NH_3; at the 75% control level, formation becomes somewhat more NH_3 controlled. That $PM_{2.5}$ nitrate levels are substantially decreased when NO_x and NH_3 are jointly reduced indicates that neither HNO_3 nor NH_3 individually dominates nitrate formation under current conditions.

Reduction of VOC and NO_x emissions to meet the proposed new standards for O_3 and PM in those areas that are in violation will require expenditures of billions of dollars. Control strategies need to account for the intricate coupling that exists between O_3 and PM. The results presented here indicate that control of gas-phase VOC and NO_x precursors generally does not lead to proportionate reductions of the secondary components of ambient particulate matter.

REFERENCES AND NOTES

1. National Research Council, *Rethinking the Ozone Problem in Urban and Regional Air Pollution* (National Academy Press, Washington, DC, 1991).
2. J. Schwartz, D. W. Dockery, L. M. Neas, *J. Air Waste Manage. Assoc.* **46**, 927 (1996); B. Brunekreef, D. W. Dockery, M. Krzyzanowski, *Environ. Health Perspect.* **103**, 3 (1995); X. P. Xu, J. Gao, D. W. Dockery, Y. Chen, *Arch. Environ. Health* **49**, 216 (1994); D. W. Dockery and C. A. Pope, *Annu. Rev. Public Health* **15**, 107 (1994); D. W. Dockery *et al.*, *N. Engl. J. Med.* **329**, 1753 (1993).
3. *Fed. Reg.* **61** (no. 241), 65763 (13 December 1996).
4. *EM* (Air and Waste Management Association, Pittsburgh, PA, January 1997), pp. 16–22.
5. F. M. Bowman and J. H. Seinfeld, *J. Geophys. Res.* **99**, 5309 (1994); *Atmos. Environ.* **28**, 3359 (1994).
6. W. R. Stockwell and J. G. Calvert, *Atmos. Environ.* **17**, 2231 (1983).
7. A. S. Wexler, F. W. Lurmann, J. H. Seinfeld, *ibid.* **28**, 531 (1994).
8. S. N. Pandis and J. H. Seinfeld, *J. Geophys. Res.* **94**, 1105 (1989).
9. A. W. Stelson, S. K. Friedlander, J. H. Seinfeld, *Atmos. Environ.* **13**, 369 (1979); A. S. Wexler and J. H. Seinfeld, *ibid.* **24A**, 1231 (1990); *ibid.* **26A**, 579 (1992).
10. J. R. Odum *et al.*, *Environ. Sci. Technol.* **30**, 2580 (1996); J. R. Odum, T. P. W. Jungkamp, R. J. Griffin, R. C. Flagan, J. H. Seinfeld, *Science* **276**, 96 (1997).
11. W. R. Pierson *et al.*, *Atmos. Environ.* **22**, 1657 (1988); A. G. Russell *et al.*, *Environ. Sci. Technol.* **27**, 2772 (1993).
12. C. I. Davidson and Y. L. Wu, in *Acid Precipitation*, S. E. Lindberg *et al.*, Eds. (Springer-Verlag, Berlin, 1989), vol. 3, pp. 103–216.
13. J. H. Seinfeld, *J. Air Pollut. Control Assoc.* **38**, 616 (1988).
14. The first three-dimensional, gas-aerosol, urban-scale model was that of C. Pilinis and J. H. Seinfeld [*Atmos. Environ.* **22**, 1985 (1988)]. Development of the conservation equations on which the current model is based is given in (*7*). A full description of the current model used in this study, together with a detailed evaluation of the model's performance in simulating the August 1987 episode considered here, will appear in (*17*).
15. Y. P. Kim, J. H. Seinfeld, P. Saxena, *Aerosol Sci. Technol.* **19**, 157 (1993); *ibid.*, p. 182.
16. D. R. Lawson, *J. Air Waste Manage. Assoc.* **40**, 156 (1990); J. C. Chow *et al.*, *Environ. Monit. Assess.* **30**, 49 (1994); J. C. Chow *et al.*, *Atmos. Environ.* **28**, 2061 (1994).
17. Z. Meng, D. Dabdub, J. H. Seinfeld, *J. Geophys. Res.*, in press.
18. R. A. Harley, A. G. Russell, G. J. McRae, G. R. Cass, J. H. Seinfeld, *Environ. Sci. Technol.* **27**, 378 (1993).
19. We would like to acknowledge support by the Electric Power Research Institute, the IBM Environmental Research Program, the U.S. Environmental Protection Agency Center on Airborne Organics, the State of California Air Resources Board, and NSF.

29 April 1997; accepted 17 June 1997